THE E896 EXPERIMENT
SEARCH FOR THE H-DIBARYON

ELEANOR G. JUDD
Mailstop 5041
Lawrence Berkeley Laboratory, 1 Cyclotron Road, Berkeley, CA 94720, USA

for the E896 Collaboration:

BNL–CERN–CMU–Catania–Goddard–Johns Hopkins–LBL–McGill–
Michigan–Ohio–Rice–UC Berkeley–UCLA–UT Austin–Wayne State–Yale

ABSTRACT

E896 is a new experiment at the Brookhaven AGS, due to take its first data in December 1996. The experiment is designed to make a sensitive search for the proposed short-lived H-dibaryon by detecting a number of possible decay channels. Two complimentary detector sets will be used: a large acceptance, slow, silicon drift detector array and a small acceptance, fast, distributed drift chamber. Time-of-flight walls and a neutron detector will be used for particle identification. The experiment motivation and design will be presented with estimates for detection efficiencies and data rates.

1. Introduction

The possibility of a stable six-quark state was first proposed by Jaffe [1] in 1977 using the MIT bag model. For a fixed number of quarks in a bag, all in the ground state, the bag states are determined by the colour-magneto interactions between the quarks. The most deeply bound state will have the most symmetic color-spin configuration, and the most anti-symmetic flavour configuration. For the $A = 2$ system these considerations lead to the prediction of a lightly bound, but stable, strange di-baryon. This six-quark state has the composition $uuddss$, baryon number $B = 2$, strangeness $S = -2$ and spin-parity $J^\pi = 0^+$. It is known as the H-dibaryon. Since Jaffe's original work with the bag model many other theories have been applied to the question of the existence of the H-dibaryon. Fig. 1 shows a summary of the theoretical predictions of the H mass from a wide range of theories between 1977 and 1993 [2]. The predictions are clustered around a mass of 2.15 GeV/c^2. An H-dibaryon with a mass in this region is below the $\Lambda\Lambda$ threshold of 2.23 GeV/c^2 so it will decay weakly rather than strongly. This puts a lower limit on the lifetime of $\tau \approx 10^{-10}s$, or half the Λ lifetime. However, the mass is above the Λn threshold, at 2.06 GeV/c^2, so the decay will have $\Delta S = 1$. This puts an upper limit on the range of possible lifetimes of $\tau \approx 100$ ns. A mass in this range opens a large number of possible decay channels for the H-dibaryon. Some of these are listed in Table 1.

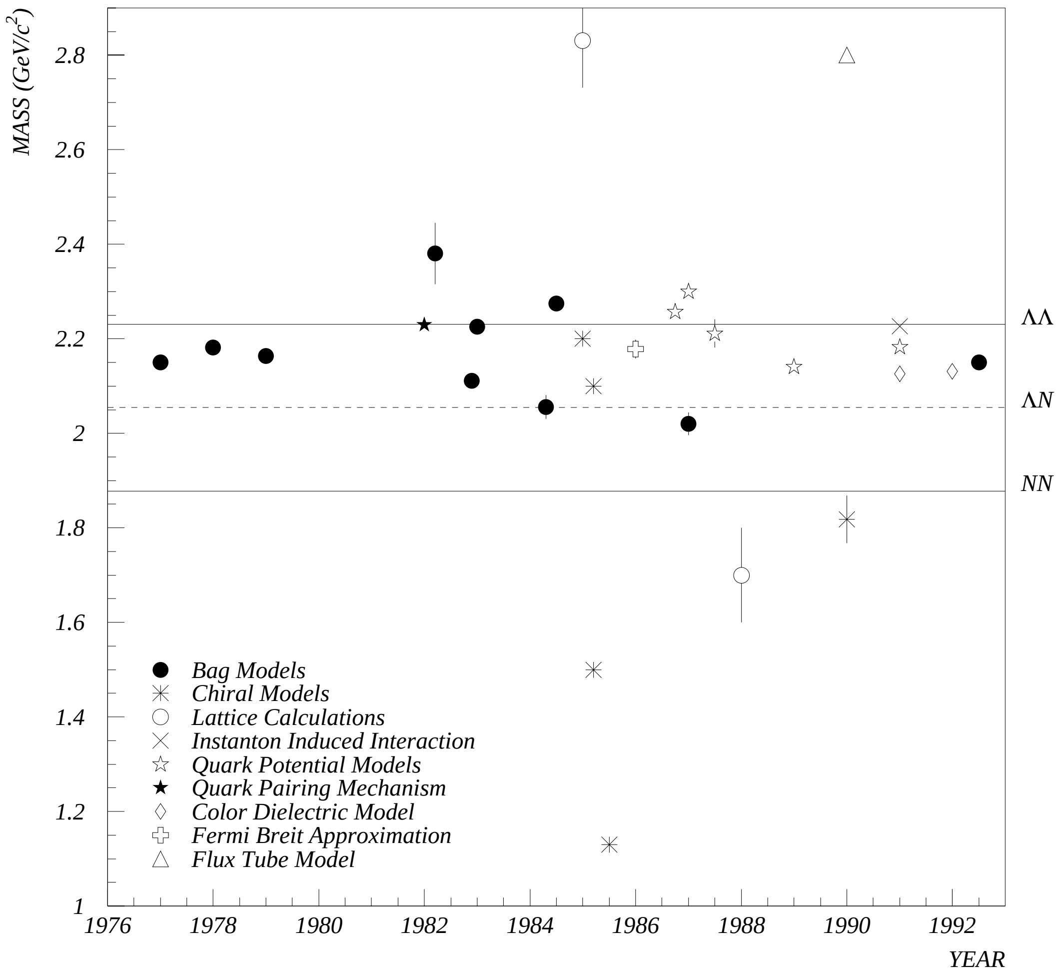

Figure 1: Theoretical predictions for the mass of the H-dibaryon as a function of year of prediction

Branch	Decay Chain	Branching Ratio %
1	$\mathrm{H} \to \Sigma^- p \to n\pi^- p$	30.0
2	$\mathrm{H} \to \Sigma^0 n \to p\pi^-\gamma n$	21.8
3	$\mathrm{H} \to \Sigma^0 n \to nn\gamma\gamma\gamma$	12.2
4	$\mathrm{H} \to \Lambda n \to p\pi^- n$	10.3
5	$\mathrm{H} \to \Lambda\Lambda \to p\pi^- n\pi^0$	9.2
6	$\mathrm{H} \to \Lambda\Lambda \to pp\pi^-\pi^-$	8.3
7	$\mathrm{H} \to \Lambda n \to nn\pi^0$	5.7
8	$\mathrm{H} \to \Lambda\Lambda \to n\pi^0 n\pi^0$	2.5

Table 1: Decay chains, and their branching ratios, for an H-dibaryon with a mass of 2.20 GeV/c^2

Figure 2: Schematic Diagram of the E896 Experimental Layout

The precise values of the branching ratios will depend on the mass of the H-dibaryon and the details of its internal structure. Experiment 896 has been designed to conduct a sensitive search for a short-lived H-dibaryon by detecting multiple decay channels. A consequence of this design is that the experiment will also be very efficient at detecting the known strange baryons, Λs etc. It should therefore be possible to perform a detailed study of Λ production systematics: Λ polarization, $\Lambda\Lambda$ correlations, and the production of other strange particles.

2. Experiment Layout

A schematic diagram of the E896 setup is shown in Fig. 2. The heart of the system is a pair of dipole magnets: the sweeper and the analyzing magnets. The upstream sweeper magnet is a new superconducting dipole magnet that has just been built by Oxford Instruments. It has a maximum field of 6.8 Tesla and an $\int B.dl$ of 4.7 Tm. The magnet bore is 15 x 50 x 122 cm. This gap will contain the target, an array of silicon drift detectors, a multiplicity counter for triggering and a collimator to shield the downstream part of the experiment. The downstream analyzer magnet is a BNL 48D48 dipole magnet. It will contain a 144 plane distributed drift chamber. The magnets are set at an angle to the beamline to optimize

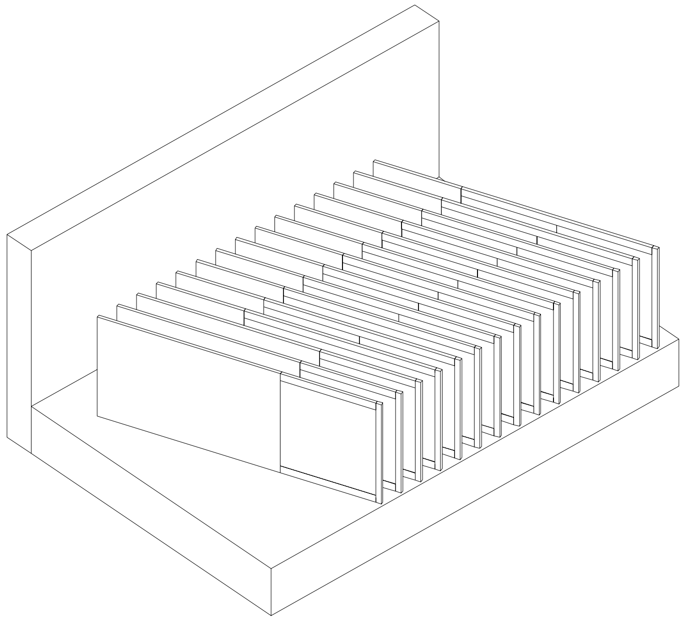

Figure 3: The E896 Silicon Drift Detector Array

the acceptance for H-dibaryon decays in this drift chamber. Downstream of the two-magnet system are 3 time-of-flight walls to identify charged particles exiting the analyzer magnet. Behind them is a neutron detector to detect the neutrons from the various H-dibaryon decay channels. Upstream of the whole system are a set of wire chambers and beam counters for triggering. In the rest of this paper the detectors used by E896 will be described in more detail.

3. Silicon Drift Detector Array

The silicon drift detector array (SDDA) is shown in Fig. 3. It is positioned inside the sweeper magnet 4.5 cm downstream of the target, where it will be sensitive to particles below mid-rapidity. In its final configuration it will consist of 15 layers of silicon detectors, of which the first 3 will be single detectors and 12 will be double detectors. These are the same detectors that will be used in the STAR Silicon Vertex Detector at RHIC. They have a position resolution of $20\mu m$ and are placed very close to the target. In this configuration simulations have shown very high tracking efficiencies can be achieved; 95 % for primary tracks and 75 % for lower momentum secondaries. The resulting momentum resolution is around 1 % for tracks with greater than 12 hits. Simulations have also been performed for reconstructing strange baryons. The results are listed in Table 2.

In the first year of data taking, 1996, only 5 detectors will be available and the DAQ speed will be limited to 1 Hz. This will severely reduce both the acceptance and efficiency for detecting strange baryons. However, in the second year, 1997, the full detector set should be available and the DAQ speed will be upgraded to 10 - 100 Hz. In this situation the SDDA

	Λ	Ξ	H0($c\tau$=4cm)
Acceptance	25 %	20 %	12 %
Efficiency	14 %	2 %	5 %

Table 2: Strange Baryon Acceptances and Efficiences in the Silicon Drift Detector Array

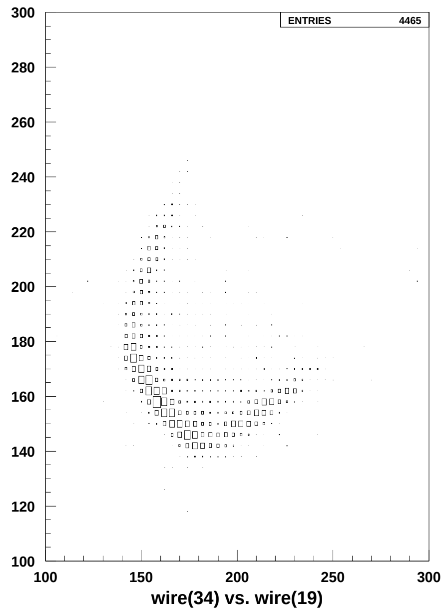

Figure 4: TDC value on an X wire vs TDC value on the nearest wire on the adjacent X$'$ plane

should reconstruct approximately 2.0 x $10^6\Lambda$s, 7000 Ξs and smaller numbers of $\overline{\Lambda}$s and ϕs.

4. Distributed Drift Chamber

The next detector system is the distributed drift chamber (DDC). This will be positioned inside the analyzing magnet, downstream of the sweeper magnet. The chamber will consist of 12 modules, each of which contains 12 planes. The orientation of the wires in these 12 planes will be $xx'uvxx'xx'u'v'xx'$. The X-planes have vertical wires and the U and V-planes are at $\pm$ 15 degrees with respect to the vertical. In the first 6 modules the planes each have 64 wires, with a cell size of 4×6 cm. The last 6 modules have 48 wires per plane and a cell size of 8×8 cm. Three full-size prototype planes were tested in the analyzer magnet in June 1996 using a proton beam. The data shows the effects of running a drift chamber in a magnetic field as shown in Fig. 4. This is a plot of the TDC value on an X-plane wire vs the TDC value on the nearest wire in the adjacent X$'$ plane for straight-through tracks. When the trajectory passes between the two wires TDC(X) is inversely proportional to TDC(X$'$).

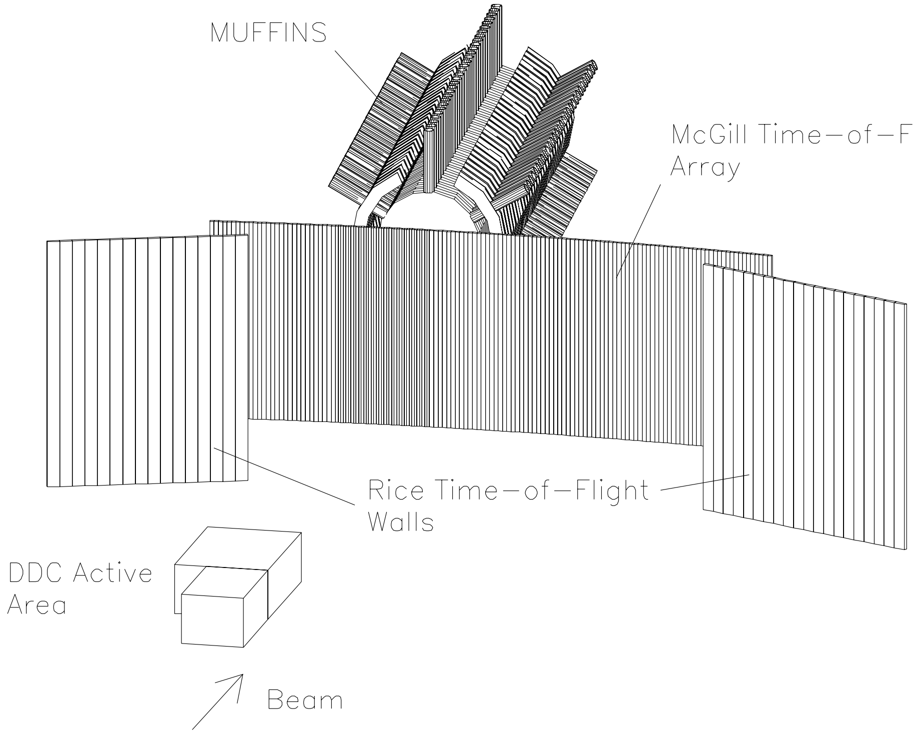

Figure 5: Time-of-flight Walls and MUFFINS with the DDC Active Area

This is the mid-section of the data in Fig. 4, and it is the only relationship that is seen in the absence of a magnetic field. The two arms in the upper and lower parts of Fig. 4 are formed when a particle traverses the planes to the left, or right, of both wires in the presence of a magnetic field. This behaviour is very nicely described by the DDC simulations software, which makes it very useful for predicting the detector response and developing analysis software. Since the DDC is much further from the target than the SDDA, its acceptance for $c\tau$=4cm H-dibaryons is much lower at 0.06 % as compared to 12 % for the SDDA. However, another effect of increasing distance from the target is that the track density decreases and track finding efficiencies increase. The efficiency for finding an H-dibaryon in the DDC is greater than 10 %, at least twice that seen in the SDDA. Finally, the DDC data acquisition rate is 1000 events/spill, faster than the SDDA DAQ rate. So, the DDC will be able to make a very sensitive search for the H-dibaryon. Any H-dibaryons that are detected will be in the mid to high rapidity range, owing to the distance from the target to the DDC. Since the SDDA covers the low to mid rapidity region the two detectors will measure adjacent, complimentary, regions of phase-space.

5. Particle Identification

The DDC measures the momentum of charged particles traversing the chamber. Another set of detectors is needed to identify these particles. The charged particles will be identified using three time-of-flight walls. Neutrons will be identified using the MUlti-Functional Neutron detector - MUFFINS. These detectors are shown in Fig. 5. There are three time-of-flight walls. The central wall is an existing wall, built by McGill University and used in experiment E877. It has 147 80x1.5 cm slats whose width varies between 1.0 and 1.7 cm. The timing resolution is 80 ps. The two outer walls are being constructed by Rice University. They both have slats measuring 5x100x1.5 cm and a timing resolution of around 100 ps. These walls have been positioned to optimize their acceptance for the various H-dibaryon decay products, as well as the decay products of known strange baryons, e.g Λs, etc. The MUFFINS detector is also an existing piece of aparatus [3], designed and built at Catania University. It consists of 30 disks of scintillator, 20 cm in radius, each of which has 6 photomultiplier tubes to detect the neutron signal. The differences in timing between the 6 signals on one disk will give the position at which the neutron hit that disk. By detecting the neutron in multiple disks its momentum vector can be determined. This information can be used to see if the neutron comes from an H-dibaryon decay detected in the DDC.

6. Conclusions

Experiment 896 is designed to detect multiple decay modes of the H-dibaryon. The experiment has two complimentary detector sets. The silicon drift detector array has a large acceptance from low to mid rapidity. It can identify charged particles from their energy loss in the silicon. However, the data rate is rather low. The distributed drift chamber covers the mid to high rapidity region. Charged particles can be identified from their time-of-flight, and neutrons are seen by the MUFFINS detector. These three constitute a high-rate detector set. Both sets of detectors are also sensitive to the known strange baryons in overlapping regions of phase space. Measurements of these particles can be used to investigate strangeness production in a relativistic heavy ion collision. They can also be used for consistency checks between the two detector sets. The first data taking will be in December 1996 and January 1997, with another run at the end of 1997. First results can be expected early in 1997.

7. References

1. R.L. Jaffe, Phys. Rev. Lett. **38**, 195 (1977)

2. C.B. Ware, Ph.D Thesis, University of Texas-Austin (December 1995); F. Merrill, Ph.D Thesis, Carnegie Mellon University (June 1995); I.R. Sukaton, Ph.D Thesis, Carnegie Mellon University, (April 1995); J.R. Klein, Ph.D Thesis, Princeton University, Princeton HEP9409 (June 1994); E. Albertson, Ph.D Thesis, Ruprecht-Karls-Univeritat Heidelberg (October 1993).

3. S. Albergo *et al.*, Nucl. Inst. and Methods **A311**, 280 (1992)